Supplementary Material

Fig. S1: Resonance scattering spectra of a 5.0 μM solution of TO-PRO-3 with varying concentrations of calf thymus DNA at 7 ^{o}C. In (A), the concentration of base pairs is increased (0, 0.9, 1.8, and 2.7 μM), and the scattering associated with the 514 nm transition increases, as indicated by the arrow. Note that the lack of significant scattering in the absence of DNA, as designated by the dotted line. In (B), higher concentrations of base pairs (3.6, 4.5, 5.3, 7.1, and 8.9 μM) result in a decrease in the intensity at 514 nm. Over a comparable concentration range, a peak at 584 nm is present in the visible absorption and circular dichroism spectra (Fig. 2B and 3B), but no enhanced resonance scattering is observed , suggesting the TO-PRO-3 molecules in Complex II interact over a shorter range than in Complex I.

Fig. S2: Visible absorption spectra during the titration of a 5.6 μM solution of TO-PRO-3 with bacteriophage T4 DNA at 7 ^{o}C. In (A), the concentration of base pairs is increased (0, 0.7, 1.6, 2.5, and 3.4 μM), which results in an increase and a decrease in the absorbances of the 514 nm and 632 nm peaks, respectively, as indicated by the arrows. In (B), the concentration of base pairs increases (3.8, 4.7, 5.8, and 7.1 μM), which results in a decrease in the absorbance of the 514 nm peak and an increase in the absorbances of both the 584 nm and 642 nm peaks. Higher base pair concentrations cause the absorbance of the 584 nm peak to decrease, while the absorbance of the 642 nm peak increases. The similarities of the spectra for T4 and calf thymus DNA suggest that major groove binding is not significant for the TO-PRO-3/DNA complexes.

Fig. S3: Visible absorption spectra during the titration of a 4.4 μM solution of TO-PRO-3 with poly(dGdC)$_2$ DNA at 7 ^{o}C. In (A), the concentration of base pairs increases (0, 0.5, 1.2, 1.9, and 3.0 μM), which results in an increase and a decrease in the absorbances of the 514 nm and 632 nm peaks, respectively, as indicated by the arrows. In (B), the absorbance of the 514 nm peak decreases at higher base pair concentrations (4.2, 5.8, 7.4, 9.7, and 14.2 μM), while the absorbance of the 642 nm band increases. Higher base pair concentrations cause the absorbance of the 584 nm peak to increase. Note that over comparable concentration ranges, a band at 584 nm is observed for poly(dIdC)$_2$ (Fig. 4S-B) but not for poly(dGdC)$_2$.

Fig. S4: Visible absorption spectra during the titration of a 4.6 μM solution of TO-PRO-3 with poly(dIdC)$_2$ DNA at 7 ^{o}C. In (A), the concentration of base pairs increases (0, 0.6, 1.3, and 2.0 μM), which results in an increase and a decrease in the absorbances of the 514 nm and 632 nm peaks, respectively, as indicated by the arrows. In (B), the concentration of base pairs was increased further (2.8, 3.7, 4.6, and 5.5 μM), thus causing the decrease in the absorbance of the 514 nm peak. In addition, the absorbances of both the 584 nm and 642 nm peaks increase over this concentration range. Higher base pair concentrations cause the absorbance of the 584 nm peak to decrease, while the absorbance of the 642 nm peak increases. The 584

nm peak is not observed for poly(dGdC)$_2$, suggesting this electronic transition is due to the lack of the amino group in the minor groove of poly(dIdC)$_2$.

Fig. S5: Visible absorption spectra during the titration of a 5.5 μM solution of TO-PRO-3 with poly(dAdT)$_2$ DNA at 7 ^{o}C. In (A), the concentration of base pairs increases (0, 0.4, 0.9, 1.3, 1.8, 2.2, and 2.6 μM), which results in a decrease and an increase in the absorbances of the 514 nm and 632 nm peak, respectively, as indicated by the arrows. In (B), higher concentrations of base pairs (2.9, 3.6, 4.3, 5.0, and 5.7 μM) causes the decrease in the absorbance of the 514 nm band. In addition, the absorbances of the 590 nm and 640 nm bands increase with the additional DNA. Note that an additional band is observed at 674 nm. In (C), the concentration of base pairs increases (6.4, 9.1, 11.1, 13.6, 17.8 μM), resulting in the increase in the absorbance at 642 nm associated with the intercalated complex.

Fig. S6: Visible absorption spectra during the titration of a 6.2 μM solution of TO-PRO-3 with the 12 base pair oligonucleotide DNA at 7 ^{o}C. Based on the studies with the longer DNA strands, the range of base pair concentrations (0, 0.4, 0.7, 1.5, 2.2, 3.0, 3.8, 4.5, 5.3, 6.0, 7.5, 9.0, 10.5, 12.0, and 15.0 μM) is sufficient to observe Complex I and Complex II (e.g. Fig. 2A and 2B). The absence of the 514 nm peak for this short oligonucleotide indicates that the stability of Complex I depends on the length of the DNA template.

Fig. S7: Circular dichroism spectra during the titration of a 5.0 μM solution of TO-PRO-3 with poly(dAdT)$_2$ at 7 ^{o}C. In (A), the concentration of base pairs increases (0, 0.5, 1.5, 2.4 μM). The vertical line at 514 nm corresponds to the absorption maximum in Fig. 5S(A). The arrows indicate that the circular dichroism associated with Complex I increases. In (B), the concentration of base pairs increases further (3.0, 3.6, 4.2, 4.8 μM), resulting in a decrease in the circular dichroism associated with Complex I. The vertical lines at 590 nm and 674 nm correspond to the absorption maxima in Fig. 5S(B), and the circular dichroism associated with these species increases over this concentration range. In (C), the concentration of base pairs increases (6.0, 8.2, 9.3, 11.5, 16.6 μM), resulting in decreases in the responses associated with the electronic absorptions at 590 and 690 nm. The vertical line at 640 nm corresponds to the intercalated complex in Fig. 5S(C). In addition, the circular dichroism response for this species increases at these higher DNA concentrations.

(A)

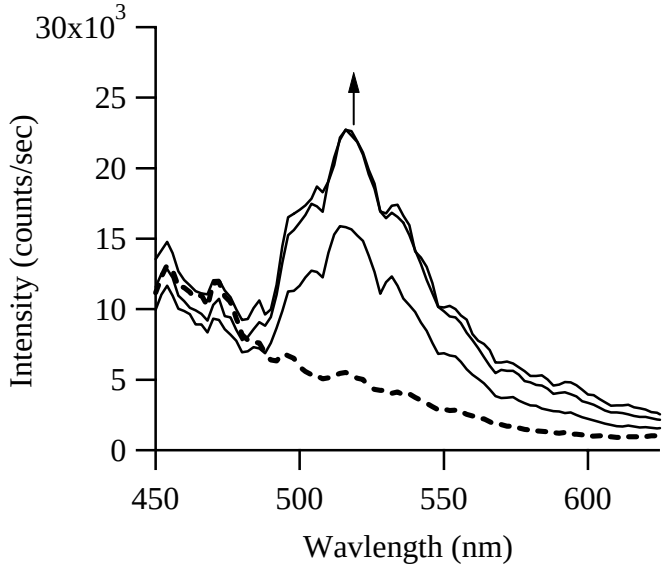
30x10^3
25
20
15
10
5
0
Intensity (counts/sec)
450
500
550
600
Wavlength (nm)

(B)

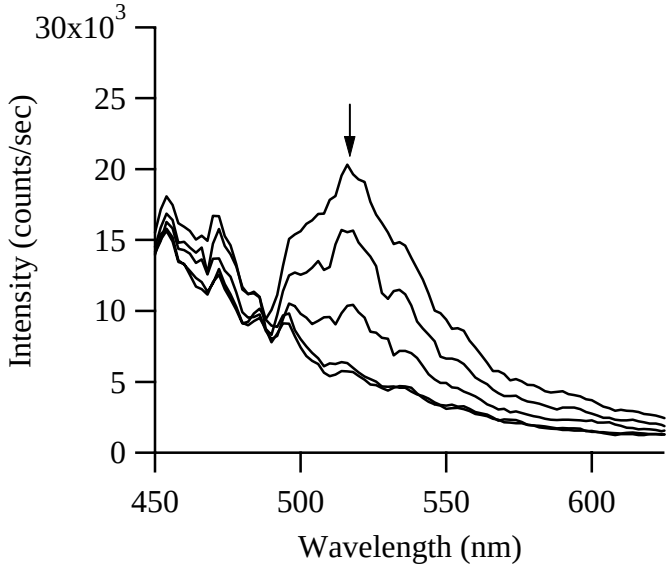
30x10^3
25
20
15
10
5
0
Intensity (counts/sec)
450
500
550
600
Wavelength (nm)

Fig. S1

(A)

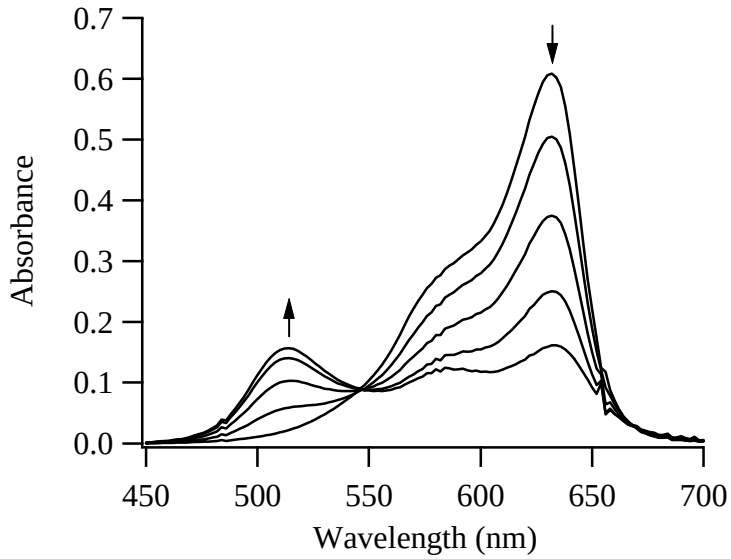
0.7
0.6
0.5
0.4
0.3
0.2
0.1
0.0
Absorbance
450
500
550
600
650
700
Wavelength (nm)

(B)

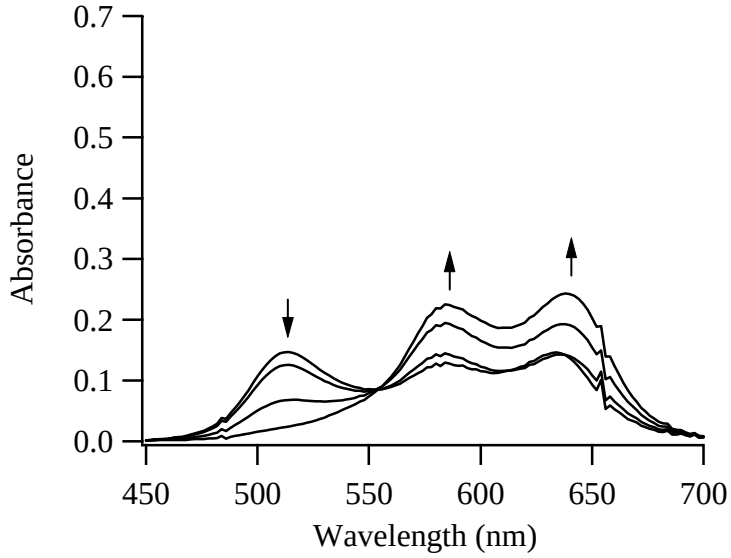
0.7
0.6
0.5
0.4
0.3
0.2
0.1
0.0
Absorbance
450
500
550
600
650
700
Wavelength (nm)

Fig. S2

(A)

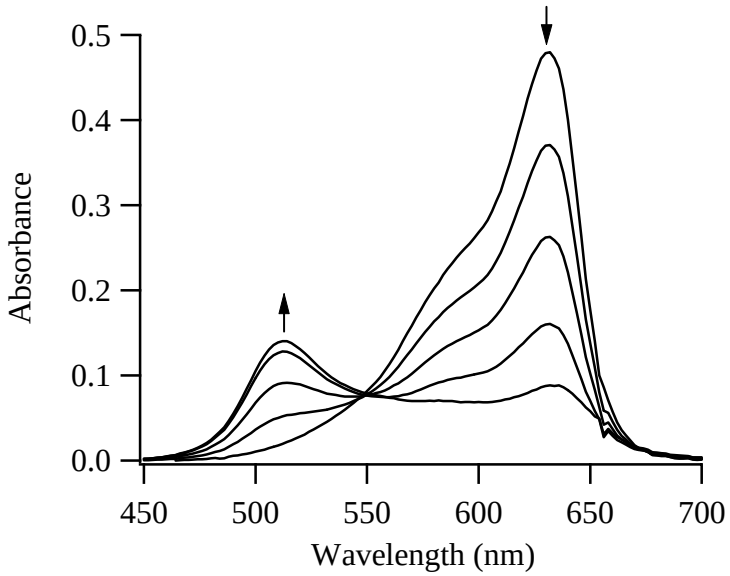
0.5
0.4
0.3
0.2
0.1
0.0
Absorbance
450
500
550
600
650
700
Wavelength (nm)

(B)

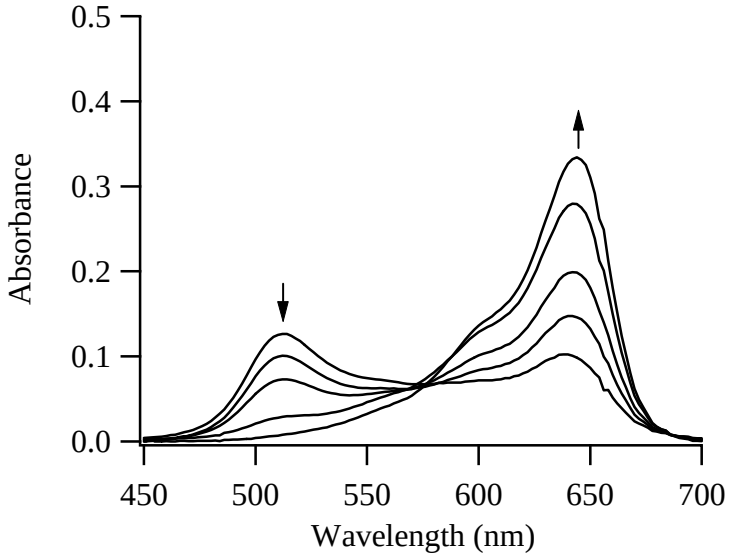
0.5
0.4
0.3
0.2
0.1
0.0
Absorbance
450
500
550
600
650
700
Wavelength (nm)

Fig. S3

(A)

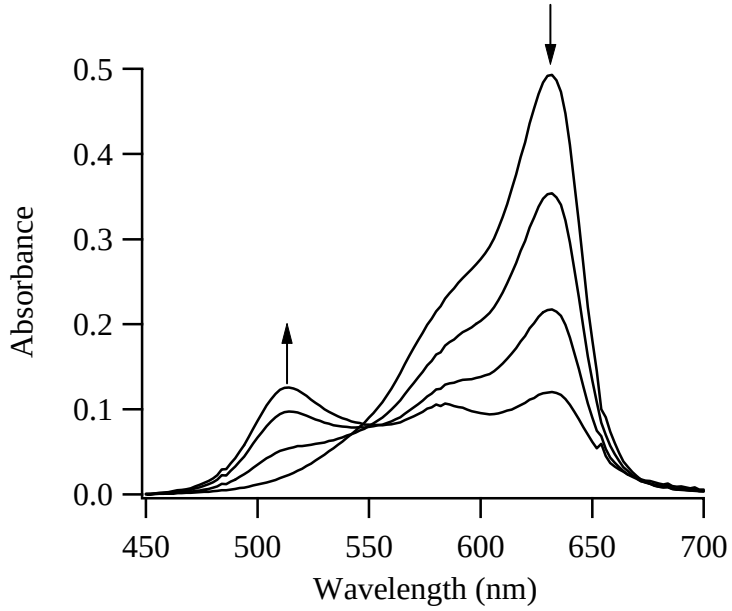
Absorbance
0.0
0.1
0.2
0.3
0.4
0.5
450
500
550
600
650
700
Wavelength (nm)

(B)

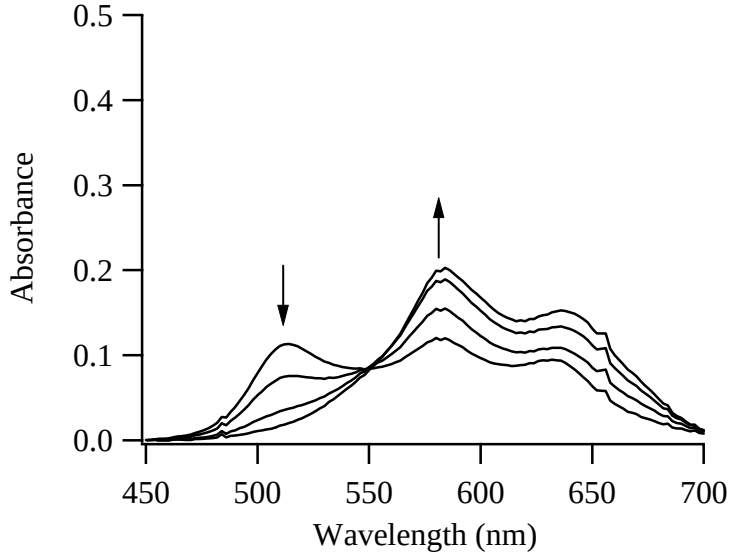
Absorbance
0.0
0.1
0.2
0.3
0.4
0.5
450
500
550
600
650
700
Wavelength (nm)

Fig. S4

(A)

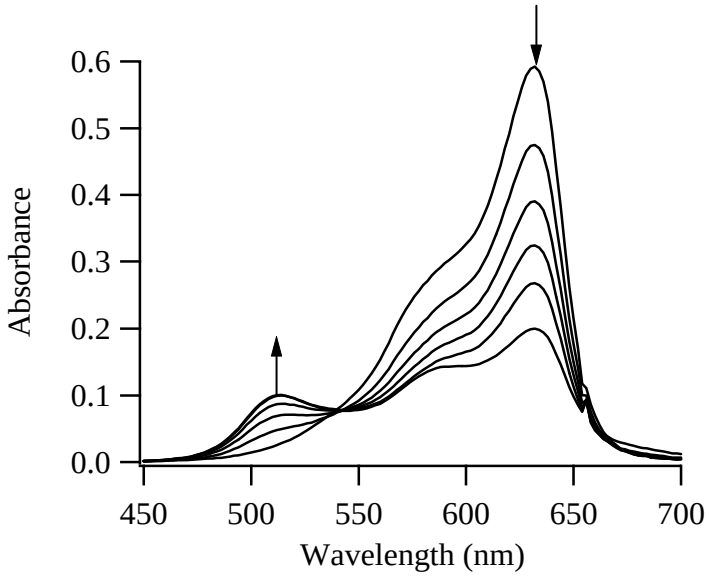
Absorbance
0.0
0.1
0.2
0.3
0.4
0.5
0.6
450
500
550
600
650
700
Wavelength (nm)

(B)

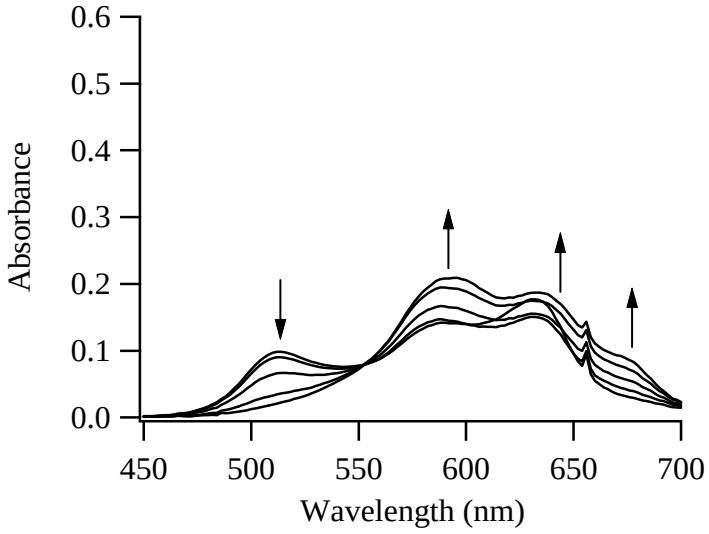
Absorbance
0.0
0.1
0.2
0.3
0.4
0.5
0.6
450
500
550
600
650
700
Wavelength (nm)

(C)

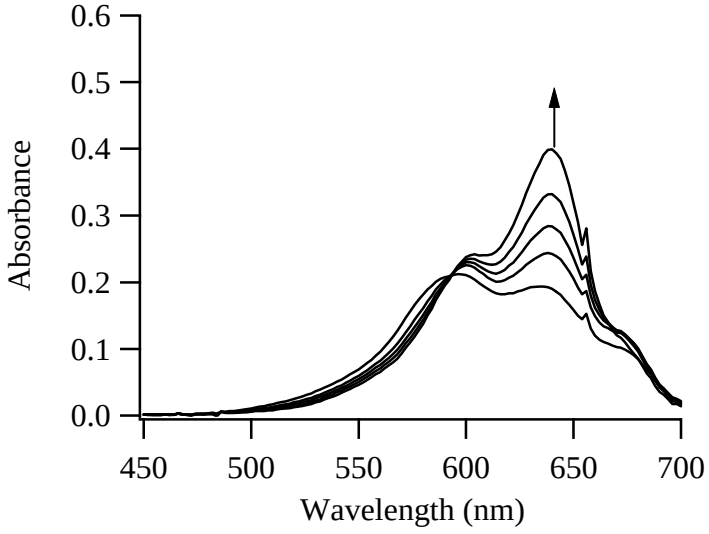
Absorbance
0.0
0.1
0.2
0.3
0.4
0.5
0.6
450
500
550
600
650
700
Wavelength (nm)

Fig. S5

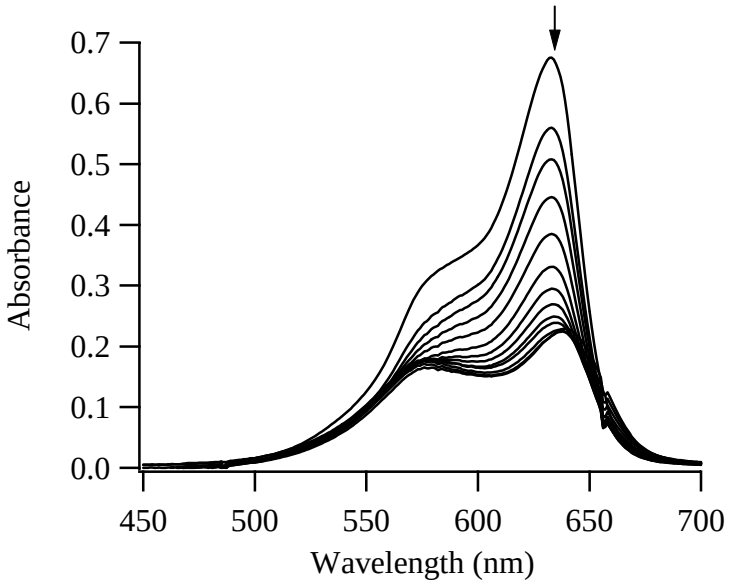
0.7
0.6
0.5
0.4
0.3
0.2
0.1
0.0
Absorbance
450
500
550
600
650
700
Wavelength (nm)

Fig. S6

(A)

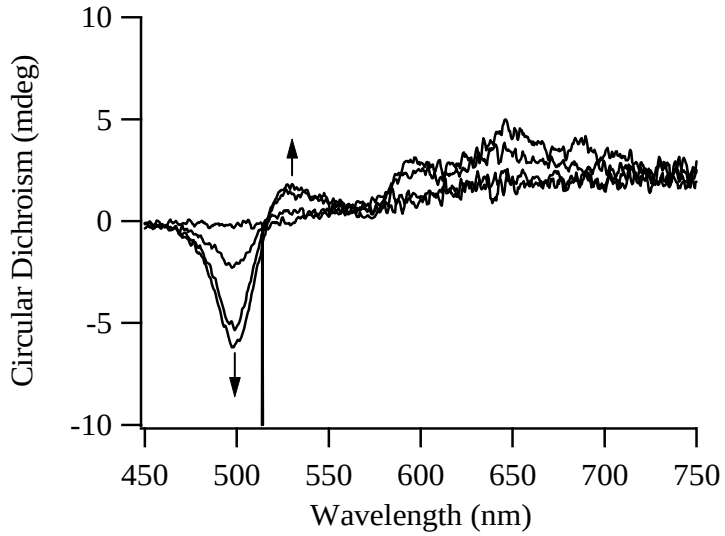
10
5
0
-5
-10
Circular Dichroism (mdeg)
450
500
550
600
650
700
750
Wavelength (nm)

(B)

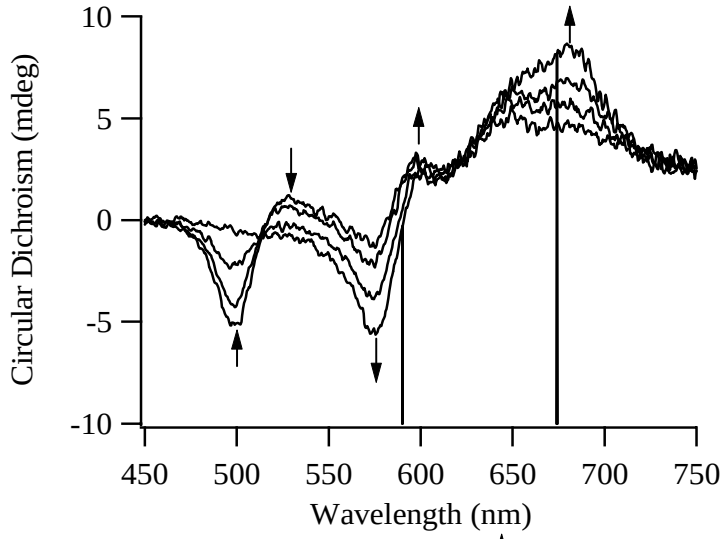
10
5
0
-5
-10
Circular Dichroism (mdeg)
450
500
550
600
650
700
750
Wavelength (nm)

(C)

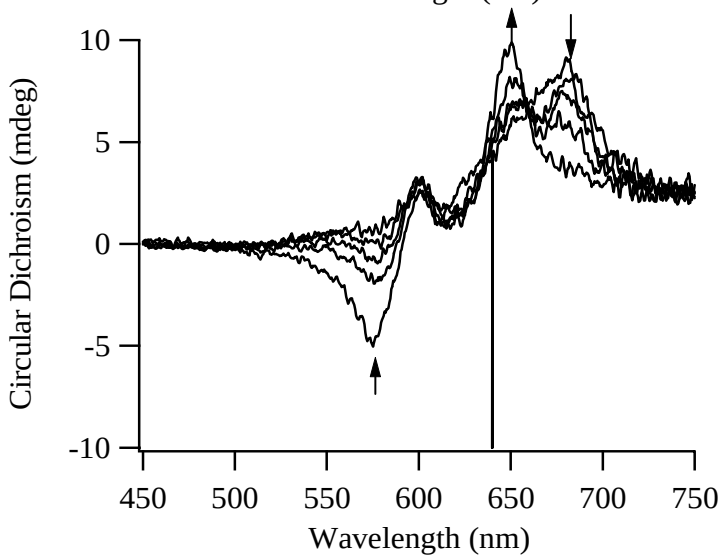
10
5
0
-5
-10
Circular Dichroism (mdeg)
450
500
550
600
650
700
750
Wavelength (nm)

Fig. S7